Clinical Epigenetics

RESEARCH

Open Access

Respiratory infection- and asthma-prone, low vaccine responder children demonstrate distinct mononuclear cell DNA methylation pathways

David Martino[1*], Nikki Schultz[1], Ravinder Kaur[2], Simon D. van Haren[3], Nina Kresoje[1], Annmarie Hoch[3], Joann Diray-Arce[3], Jessica Lasky Su[4], Ofer Levy[3,4,5], Michael Pichichero[2] and in association with the IDEAL Consortium

Abstract

Background Infants with frequent viral and bacterial respiratory infections exhibit compromised immunity to routine immunizations. They are also more likely to develop chronic respiratory diseases in later childhood. This study investigated the feasibility of epigenetic profiling to reveal endotype-specific molecular pathways with potential for early identification and immuno-modulation. Peripheral blood mononuclear cells from respiratory infection allergy/asthma-prone (IAP) infants and non-infection allergy/asthma prone (NIAP) were retrospectively selected for genome-wide DNA methylation and single nucleotide polymorphism analysis. The IAP infants were enriched for the low vaccine responsiveness (LVR) phenotype (Fisher's exact p-value = 0.02).

Results An endotype signature of 813 differentially methylated regions (DMRs) comprising 238 lead CpG associations (FDR < 0.05) emerged, implicating pathways related to asthma, mucin production, antigen presentation and inflammasome activation. Allelic variation explained only a minor portion of this signature. Stimulation of mononuclear cells with monophosphoryl lipid A (MPL), a TLR agonist, partially reversed this signature at a subset of CpGs, suggesting the potential for epigenetic remodeling.

Conclusions This proof-of-concept study establishes a foundation for precision endotyping of IAP children and highlights the potential for immune modulation strategies using adjuvants for future investigation.

Ş Full list of consortium members in Table S2.

*Correspondence:
David Martino
david.martino@telethonkids.org.au
[1] Wal-Yan Respiratory Research Centre, Telethon Kids Institute, University of Western Australia, 35 Stirling Highway, Crawley, WA 6009, Australia
[2] Centre for Infectious Disease and Vaccine Immunology, Research Institute, Rochester General Hospital, 1425 Portland Avenue, Rochester, NY 14621, USA
[3] Precision Vaccines Program, Department of Pediatrics, Boston Children's Hospital, 300 Longwood Ave, BCH 3104, Boston, MA 02115, USA
[4] Channing Division of Network Medicine and Harvard Medical School, Boston, MA 02115, USA
[5] Broad Institute of MIT and Harvard, 415 Main St, Cambridge, MA 02142, USA

Background

Respiratory infections in early life are among the leading causes of childhood morbidity and mortality and the most common cause of respiratory admissions to hospitals [1]. While vaccines can help prevent some respiratory diseases, some children exhibit a phenotype of low responsiveness to their routine schedule of vaccines [2] and are vulnerable to upper respiratory tract infections, particularly acute otitis media [3, 4]. A 10-year study of acute otitis media (AOM) children conducted in Rochester, New York, revealed that children prone to AOM, termed otitis prone (OP), exhibit sub-protective IgG antibody levels to most of their scheduled pediatric vaccine antigens [5]. Clinically, they also experience substantially higher rates of subsequent allergies and asthma [5]. Otitis-prone children are more susceptible to respiratory infections due to associated nasopharyngeal (NP) and systemic immune deficits [6, 7]. Specifically, a reduced capacity to respond to infections is associated with reduced activation of Toll-like receptor (TLR) signaling pathways and cytokine production [7], leading to attenuated stimulation of $CD4^+$ T cell responses, specifically Th17 responses to extracellular pathogens [8]. This disparity in immune development in children who suffer from high rates of otitis media, allergy and asthma constitutes a unique endotype of 'respiratory infection, allergy/asthma-prone children' (IAP) that merits focused investigation for the development of precision interventions.

Endotyping approaches to classifying diseases based on molecular and biological pathways, rather than clinical symptoms, have the potential to lead to new options for early preventative treatments [9, 10]. In this study we undertook a precision endotyping approach focused on DNA methylation biomarkers (CpG methylation) which are regulatory base modifications to DNA that influence cellular immune responses across the life course [11]. Such modifications vary according to host genotypic variation and environmental influences and therefore contain information about both genome and environment [12]. Their potential utility for endotyping is supported by studies that demonstrate respiratory infections modify host CpG methylation in both nasal tissue and blood leukocytes [13, 14].

Post-infectious epigenetic modifications to leukocyte DNA can be retained at immune response genes, a concept known as 'epigenetic scars,' and these modifications can induce cellular non-responsiveness ('tolerance'), increasing host susceptibility to severe infections and sepsis [15]. We postulated that DNA methylation profiling of PBMCs might reveal similar markers in IAP children that could be harnessed to develop endotype signatures. One feature of the 'epigenetic scars' concept is the potential to restore functionality using adjuvants that reverse specific nucleic acid base modifications [16, 17]. As part of the mission of the National Institutes of Health (NIH)/National Institute of Allergy & Infectious Diseases (NIAID) Immune Development in Early Life (IDEAL) program, we sought to identify modifiable pathways of immune development with therapeutic potential by investigating the impact of a common adjuvant on endotype-specific molecular signatures. This approach may identify molecules with the potential to redirect the course of immune development in vulnerable children away from endotypes associated with disease and toward those associated with health [18].

In this proof-of-concept study, we retrospectively selected children from a longitudinal child cohort enrolled and followed prospectively in Rochester from 6 to 60 months of age. PBMCs from 14 IAP infants collected in the first year of life were matched to 16 non-respiratory infection allergy/asthma-prone (NIAP) controls using extremes of phenotype design. Sample classifications for vaccine responsiveness determined from antibody responses to primary vaccinations were previously available on this cohort [19]. PBMCs collected from these children, were cultured with vehicle control (PBS) or with monophosphoryl lipid A (MPL) which is a TLR4 agonist. At culture endpoint, cells were harvested for methylome- and genome-wide association analysis using infinium microarray technology. Using differential analysis, we identified an endotype signature of epigenetic differences in unstimulated cells that was partially modifiable using MPL adjuvant following in vitro stimulation.

Results

Study participant characteristics

The characteristics of the participants are presented in Table 1. The IAP group consisted entirely of Caucasian ancestry, whereas the NIAP group comprised 81% Caucasians and 19% other ethnicities. Principal component analysis (PCA) of genotypes confirmed that the study cohort was predominantly of Caucasian ancestry, with three individuals clustering with middle clines reflecting Latino and African-American ancestry components (Additional file 1: Fig. S1). The IAP group were enriched with the low vaccine responder (LVR) phenotype (Fisher's exact p-value = 0.02) and had a higher burden of stringently defined otitis media (Fisher's Exact p-value < 0.001).

Epigenome-wide association study of endotype-linked methylation patterns

We conducted an epigenome-wide association study (EWAS) comparing unstimulated (PBS) mononuclear cells from IAP infants vs. NIAP infants. This analysis identified 813 differentially methylated regions

Table 1 Demographics of study cohort

Variable	Category	IAP	NIAP	Overall	*P*-value
Vaccine responsiveness					0.019
	High vaccine response	(1) 7%	(5) 31%	(6) 20%	
	Normal vaccine response	(6) 43%	(10) 62%	(16) 53%	
	Low vaccine response	(7) 50%	(1) 6%	(8) 26%	
Otitis-prone status					< 0.001
	Stringently defined otitis prone	(10) 71%	(0) 0%	(10) 33%	
	Non-otitis prone	(4) 29%	(16) 100%	(20) 67%	
Atopy					0.675
	Eczema	(4) 29%	(3) 18%	(7) 23%	
Sex					0.44
	Female	(3) 21%	(6) 38%	(9) 30%	
	Male	(11) 79%	(10) 62%	(21) 70%	
Age (months)	Mean	9.9 ± 2	10.76 ± 1.59	10.36 ± 1.81	0.211
Ancestry					0.485
	African-American	(0) 0%	(1) 6%	(1) 3%	
	Caucasian	(14) 100%	(13) 81%	(27) 90%	
	Other	(0) 0%	(2) 12%	(2) 7%	
Daycare					0.142
	Yes	(11) 79%	(8) 50%	(19) 63%	
	No	(3) 21%	(8) 50%	(11) 37%	
Breastfeeding					0.883
	Breastfed	(4) 29%	(3) 19%	(7) 23%	
	Formula fed	(8) 57%	(10) 62%	(18) 60%	
	Both	(2) 14%	(3) 19%	(5) 17%	
Smokers in home					1.00
	Yes	(0) 0%	(1) 6%	(1) 3%	
	No	(14) 100%	(15) 94%	(29) 97%	
Siblings					0.457
	Yes	(7) 50%	(11) 69%	(18) 60%	
	No	(7) 50%	(5) 31%	(12) 40%	

P-values are determined using Fisher's exact for categorical variables and t-test for quantitative variables

(DMRs) encompassing 268 lead CpG associations with genome-wide significance (Fig. 1A, see Additional file 3: Table S2). Notably, most regions exhibited higher methylation (hypermethylation) in the IAP group (60.4%, 491 regions).

To assess the role of genetic variation in shaping this endotype-associated methylation signature, methylation quantitative trait loci (mQTL) analysis was performed using individual regression models for SNP-CpG pairs within a ± 500 kb window of endotype-associated CpGs (1,079,685 SNP markers). This analysis revealed 52 unique SNP associations with methylation levels at 5 CpG dinucleotides (FDR < 0.05) (Fig. 1B).

Gene ontology analysis showed enrichment for genes involved in mucin-type O-glycan biosynthesis in both hyper- and hypomethylated DMRs (Fig. 1C). Hypermethylated regions contained the genes *B3GNT3*, *B3GNT6*, *GALNT9*, *ST3GAL1*, *FUT11*. Hypomethylated regions included *GALNT2*, *GALNT18*, *GALNT9*, suggesting potential links to epithelial dysfunction [20, 21]. Notably several relevant disease pathways including asthma, diabetes, graft rejection and antigen processing pathways were enriched in hypermethylated regions. The latter involved genes within the major histocompatibility complex (class I member *HLA-F*, class II members *HLA-DPA1* and *HLA-DPB1*and protease subunit *PSMB8)* [22–24].

Additional hypermethylation was observed in genes associated with the inflammasome pathway in IAP children, including *PCSK6* [25], *NLRP1* [26], *FLT4* and *IL18RAP* [27] 28, suggesting deficits in anti-viral defenses. Furthermore, hypermethylation was also

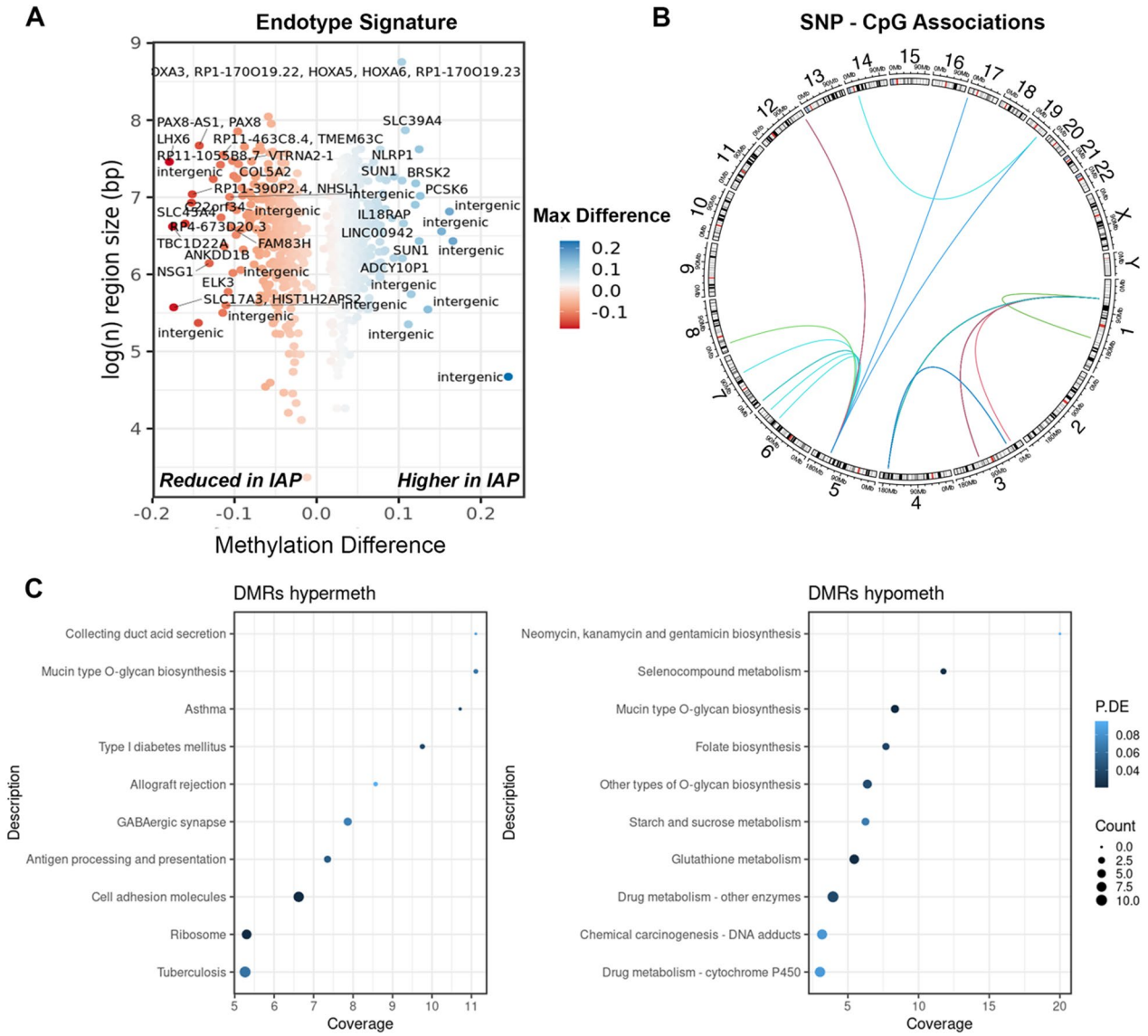

Fig. 1 Epigenome-wide association study of IAP and NIAP infants demonstrates differentially methylated regions enriched with immune response genes. **A** Volcano plot of differentially methylated regions significantly associated with IAP status. X-axis represents the average methylation change from NIAP group (delta methylation ratio), and the y-axis shows the log region size in base pairs. Points are colored according to maximum observed methylation difference in region. $N = 30$ **B** Circular visualization of significant SNP-CpG association pairs showing chromosomal location of associated markers. **C** Dot chart of summary statistics from gene ontology enrichment analysis of the infection-prone associated methylation signature highlighting significantly enriched pathways. The y-axis shows gene set nomenclature, point size reflects total count of differentially methylated genes, points are ranked by the percentage of genes in the set covered, and colored according to false discovery rate adjusted *P*-value. *Diff* Differentially, *DMRs* differentially methylated regions, *IAP* infection allergy/asthma prone, *max* maximum, *bp* base pairs, *P.DE p*-value for over-representation of the GO or KEGG term, *Coverage* percentage of genes identified within specified pathway

observed in immune response genes including *MAP3K6*, *KSR1* [29] and *PARP9* [30], implicated in the IFN-γ response. *AKT1* involved in the PI3K/AKT/mTOR pathway [31], and *MYD88*, crucial for TLR signaling also exhibited hypermethylation [32]. Conversely, hypomethylated DMRs were primarily enriched with genes involved in cellular metabolism, such as glutathione metabolism (*GCLC*, *GSTA4* and *GSTM3)* [33], and starch and sucrose metabolism (*HK2* and *PYGB*) [34, 35] (Fig. 1A).

To decipher the cellular specificity of this endotype signature, immune cell subset deconvolution of peripheral blood methylation profiles was performed using differentially methylated cell type (DMCT) analysis [36]. This

analysis did not reveal differentially methylated cell types, suggesting a generalized signature across immune cell subsets (Additional file 1: Fig. S2).

In vitro *MPL stimulation alters DNA methylation in endotype-associated genes*

To explore how innate immune activation might affect disease-linked methylation patterns, PBMCs from the same study participants were stimulated with MPL for 24 h and analyzed via EWAS. Compared to PBS-treated cells, MPL stimulation induced modest methylation changes (average effect size ~ ± 5%) in 113 regions (FDR < 0.05), encompassing both hypermethylation (60 regions) and hypomethylation (53 regions). Immune cell-type distributions remained unchanged after stimulation (Additional file 1: Fig. S2, Additional file 4: Table S3).

Gene ontology analysis revealed enrichment of similar pathways as the endotype signature (e.g., asthma, type 1 diabetes) and additional pathways linked to inflammasome signaling (NF-κB signaling, Th17 cell differentiation), suggesting the potential of MPL to target endotype-associated methylation (Fig. 2A). A modest but significant overlap ($P = 0.002$ hypergeometric test) between endotype- and stimulation-associated regions was detected (Fig. 2B). Interestingly, 183 of 268 significant CpGs differentiating NIAP and IAP groups lost significance after MPL treatment (FDR P ≥ 0.05), indicating specific methylation pattern modulation by MPL.

Bland–Altman visualization (Fig. 2C) confirmed effect size modulation on inter-group methylation variability. Notably, 8 CpGs displayed > 5% modulation of the IAP-NIAP group difference by MPL stimulation (FDR $P < 0.05$, interaction test, Fig. 2D).

Discussion

This study introduces a novel approach to identifying children vulnerable to respiratory infections and low vaccine responsiveness through precision epigenetic endotyping. This approach holds potential to revolutionize early detection and guide targeted interventions, ultimately improving immune resilience and preventing chronic disease in this at-risk group. Aligning with the NIH/NIAID's IDEAL consortium mission, our work aims to personalize immunizations and prevent infectious diseases in early life by combining disease- and adjuvant-associated molecular signatures to identify molecules capable of reversing disease pathways. These results pave the way for larger-scale validation studies with the hope of personalized immunotherapies, transforming healthcare for children at high risk of severe respiratory illnesses.

Children within this long-term Rochester cohort experiencing a high burden of recurrent infections in their first five years of life [37] exhibited a distinct molecular signature in mononuclear immune cells collected during infancy. This endotype signature was characterized by increased methylation in genes governing pro-inflammatory immune responses including inflammasome formation, antigen processing and glycan biosynthesis. This suggests a potential role in heightened susceptibility to respiratory infections [20, 38]. While our analysis indicated minimal influence from genetic risk variants, implying the disease signature reflects more of a developmental programming element, further studies with larger sample sizes are needed to solidify this conclusion.

Notably, this study demonstrates the ability of our methylation profiling approach to identify clinically relevant signatures that corroborate existing clinical and immunological findings in IAP children [2, 4, 6, 7, 39–43]. For example, we observed increased methylation at several MHC genes, consistent with the previous reports of reduced surface expression of MHC II proteins in this population [2]. Additionally, our findings regarding increased methylation in *MyD88*, a key component of PRR-mediated signaling, align with previous observations of reduced IRF7 mRNA expression and IFN-α production [2, 8, 41, 44]. Similarly, increased methylation of inflammasome-related genes (*NLRP1, IL18RAP, PCSK6, FLT4)* in IAP children is consistent with reduced IL-1β-mediated T-helper 17 immunity reported in children prone to AOM [8].

While increased methylation at identified genes suggests potential dysregulation in relevant pathways, the functional consequences require further investigation. Hypermethylation often impedes DNA accessibility, potentially reducing gene expression and contributing to the IAP phenotype [45]. However, the context-dependent nature of methylation necessitates additional functional follow-up studies. Importantly, it is critical to recognize that the observed changes may not reflect causal drivers but could also arise from gene–environment interactions or disease manifestations.

While our findings reveal minimal overall overlap between endotype- and stimulation-associated methylation patterns, the selective modulation of 8 CpGs by MPL suggests its potential to fine-tune methylation landscapes and potentially influence downstream transcriptional and functional pathways. It remains unclear how MPL modulates endotype-associated pathways, and limited insights can be gleaned from bulk epigenetic data. Further investigations using single-cell epigenetic analysis and functional assays will be needed to define the pathways by which adjuvants impact their target genes. Developing a computational epigenetic signatures database could provide a valuable resource

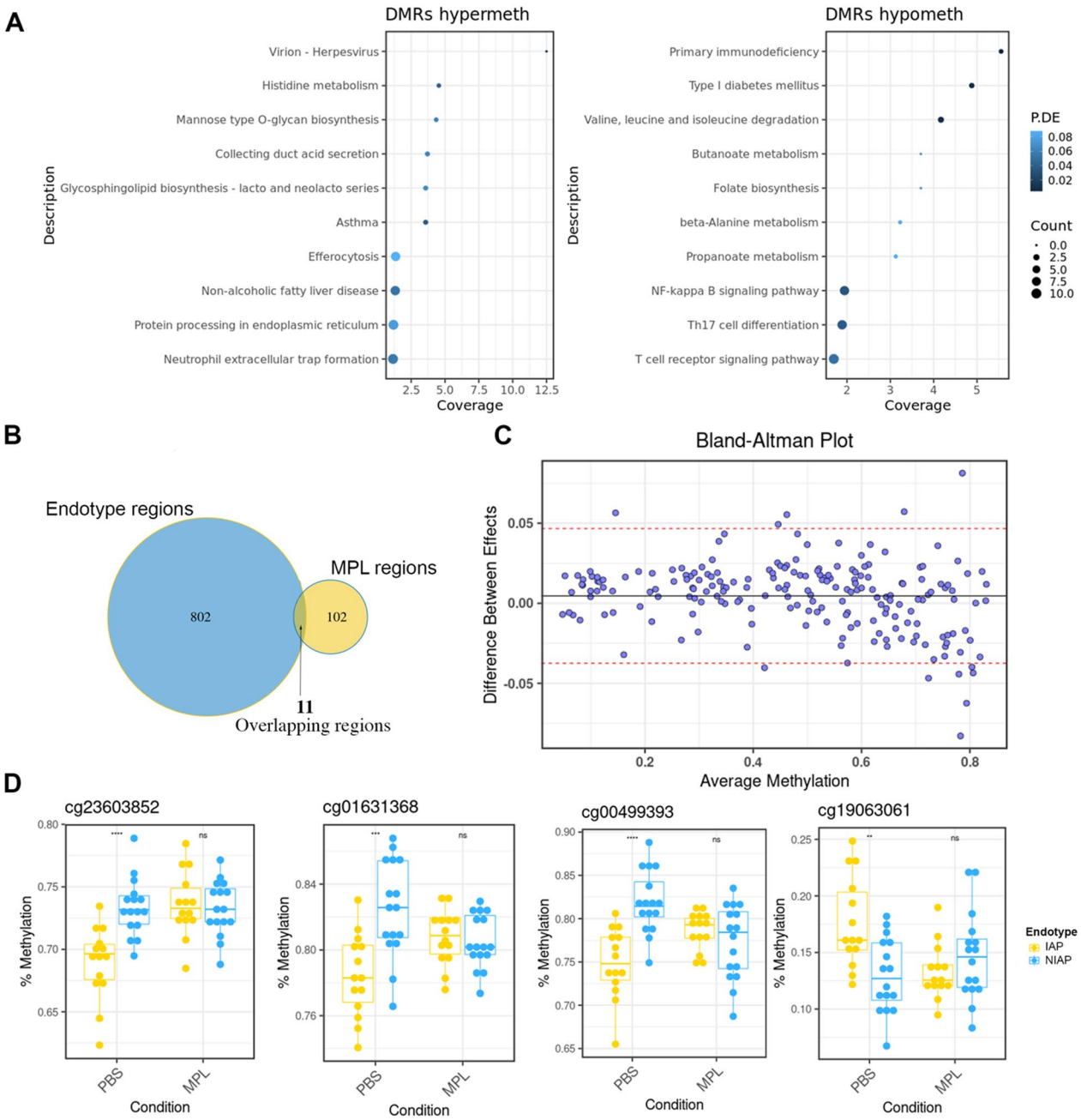

Fig. 2 Stimulation with MPL adjuvant modifies a subset of endotype-associated CpGs. **A** Dot chart of summary statistics from gene ontology enrichment analysis for the MPL-associated differentially methylated regions highlighting significantly enriched pathways ($n = 30$). The y-axis shows gene set nomenclature, point size reflects total count of differentially methylated genes, points are ranked by the percentage of genes in the set covered, and colored according to false discovery rate adjusted *P*-value. **B** Venn diagram of overlapping regions showing counts of unique and overlapping regions. **C** Bland–Altman visualization of methylation difference after MPL stimulation for 183 MPL-sensitive CpGs. Y-values represent the difference in log2 fold-change (NIAP – IAP) between PBS and MPL condition. X-axis shows mean methylation value for each CpG. Upper and lower 95% confidence intervals are shown as red lines. **D** Boxplot of median and quartile range for the four most significantly ranked endotype-associated CpGs modified by MPL treatment. *DMRs* differentially methylated regions, *MPL* monophosphoryl lipid A, *P.DE p*-value for over-representation of the GO or KEGG term, *Coverage* percentage of genes identified within specified pathway. *Hypermeth* hypermethylated regions. *Hypometh* hypomethylated regions.*** = $P < 0.001$, ** = $P < 0.05$–0.05, ns = $P > 0.05$, two-sided t-test

for precision immunization approaches in vulnerable populations and a starting point for pre-clinical studies.

This was a proof-of-concept study with some caveats, including a small and highly selected sample group and a lack of functional studies. We utilized an extremes of phenotype design; while this approach does not provide a perfectly representative sample of the entire cohort, it is a common strategy in pilot studies, aiming to maximize the contrast between groups and increase the likelihood of detecting meaningful differences when the sample sizes are small. This study establishes the foundation for future research into a precision epigenetic endotyping approach, potentially improving health outcomes in children at high risk for respiratory illnesses.

Methods

Sample selection

Participants in a prospective trial conducted in Rochester NY, USA, were children recruited from community-based primary care pediatric practices, as previously described [5]. Infection asthma-prone (IAP) status was determined from unsupervised clustering analysis of illness visits over the first 5 years of life, described in [5]. Briefly, the frequency of illness and allergy episodes were expressed as a binary vector for each study participant, and multi-dimensional scaling (MDS) performed. Unsupervised K-means clustering was performed to illness and allergy data and identified a cluster that was highly enriched for respiratory illness. For the current study, a subset of 30 participants was selected, 14 of which were IAP cases and 16 NIAP controls. Participant selection was intentionally guided to emphasize the extremes of clinical phenotypes, that is, respiratory infection allergy/asthma-prone children (IAP) enriched for low vaccine responder (LVR) phenotype vs. non-respiratory infection allergy/asthma prone (NIAP) (Table 1). Briefly, among the IAP subset we selected study participants that were prone to otitis media as it is strongly correlated to low vaccine responsiveness (unpublished observations) with available PBMC. Among the NIAP we randomly selected study participants from those with multiple PBMC vials available. Vaccine responsiveness was determined from normalized IgG titers to six vaccine antigens measured at one year of age following their primary immunizations. LVRs are defined as the bottom 25th percentile of the geometric mean of the 6 normalized titers, as detailed in [19]. Briefly, VR was separated into three categories: low vaccine response, normal vaccine response and high vaccine response. The percentile cutoffs were determined for each age group between 6 and 36 months.

PBMC stimulation in vitro

Cryopreserved PBMCs were thawed by dropwise addition of cold RPMI 1640 medium (Gibco) supplemented with penicillin/streptomycin (Gibco), 2 mM l-glutamine (Gibco) and 10% bovine serum (Hyclone). Stimuli included Phosphate-Buffered Saline (PBS) as a vehicle control, and synthetic Monophosphoryl Hexa-acyl Lipid A, 3-Deacyl (3D(6A)PHAD, Avanti Polar Lipids), abbreviated to MPL. MPL was used at a concentration of 1 µg/mL. MPL was prepared at 10X the desired concentration, and 20 µL was added to flat-bottom sterile, pyrogen-free 96-well culture dish wells (Corning). PBMCs were washed with RPMI, counted, and viable cells determined by Trypan Blue staining (Gibco) were resuspended in RPMI supplemented with penicillin/streptomycin, 2 mM l-glutamine, and 10% autologous plasma at a concentration of 2.78 million cells/mL. 180 µL of cell suspension (500.000 PBMCs) was plated on top of stimuli. Plates were incubated for 24 h in a humidified incubator with 5% CO2. After 24 h, culture supernatants were stored at − 80 °C and cells were centrifuged for 3 min at 500 rpm. Cell pellets were resuspended in 500 µL RNAlater (Sigma-Aldrich) for downstream DNA methylation profiling and frozen at -80 degrees. Each clinical sample ($n=30$) had a vehicle-only (PBS) condition, and a matched MPL condition (total $n=60$), both cultured for 24 h.

DNA methylation profiling

PBMC pellets were thawed and washed in PBS prior to genomic DNA extraction using the Chemagic DNA 400 kit H96 (cat # CMG-1491). DNA samples were quantified using the Quant-iT HS kit (cat# Q33120) and randomized by endotype label prior to being sent to the Australian Genome Research Facility in Melbourne, Western Australia, for bisulfite conversion and genotyping using Illumina Infinium MethylationEPIC BeadChip v1 arrays. Bisulfite-converted genomic DNA was analyzed using Illumina's Infinium Human Methylation EPIC BeadChips, which enable methylation measures at over 850,000 CpG sites. Raw.iDAT files were pre-processed using the Minfi [46] package from the Bioconductor project (http://www.bioconductor.org) in the R statistical environment (http://cran.r-project.org/ version 4.2.2). Sample quality was assessed using control probes on the array, and no samples were removed. Array normalization employed the stratified quantile method to correct for type 1 and type 2 probe biases. Probes exhibiting a P-detection call rate of > 0.01 in one or more samples were removed (44,881 probes) prior to analysis. Probes containing SNPs at the single base extension site or at the CpG assay site were removed, as were probes measuring

non-CpG loci (30,015 probes). Probes reported to have off-target effects by McCartney et al. [47] were also removed (39,489 probes). After filtering, the final dataset consisted of 120 samples and 751,474 probes. Methylation ratios were derived as β values (methylated alleles)/((unmethylated + methylated) × 100)) with log2 transformation to M values for statistical analysis.

Genotyping and imputation

Aliquots of genomic DNA samples were genotyped by the Australian Genome Research Facility using the Illumina Global Screening Array v3 with a multi-disease drop-in. Genotype calling was performed using the *gencall* algorithm in GenomeStudio (Illumina). Quality control was performed using the plinkQC package (v 0.3.4) [48] to remove samples with > 5% missing data, with high relatedness (PI_HAT > 0.2) in identity-by-descent analysis for all pairs of samples, or with mismatched ancestry estimates based on principal component analysis of merged data with the 1000 genomes phase 3 dataset. We also excluded SNPs characterized by > 5% missing values, a Hardy–Weinberg equilibrium p-value < 0.001 and a minor allele frequency of < 5%. Quality-controlled data were then imputed with the Haplotype Reference Consortium hg19 r1.1 reference panels using Beagle 5.4 on the Michigan imputation server. Imputed genotypes were filtered to remove SNPs with a minor allele frequency of < 5% and Hardy–Weinberg equilibrium *p*-value < 0.001, with an r2 value > 0.3.

Statistical analysis

Linear regression modeling employed the R statistical environment using the limma package [49] to test the association between DNA methylation, IAP status and stimulation conditions. A factorial model with main effects on disease status and stimulation, including covariate adjustment for cell-type proportions, the 1st five principal components of the methylation dataset, 1st two principal components of the SNP dataset, sex and age, was fitted to the methylation ratios (M-values). We used the corfit function to adjust the variance estimates for the repeated-measures samples. To determine endotype-specific signatures, we compared unstimulated samples for the main effect of disease status adjusted for covariates. Summary statistics from the model fit were used to identify differentially methylated regions (DMR) using the R package DMRcate [50]. DMRs were defined using a lambda of 1000, min. cpgs of 4 and adjusted p-cutoff of 0.05. To derive stimulus-specific signatures, we compared each stimulation with the unstimulated control samples, adjusting for disease status and covariates. Gene ontology enrichment analysis of all differentially methylated regions was conducted using the missMethyl R package [51]. Cell-type proportions and deconvolution were estimated using the EpiDish (Epigenetics Dissection of Intra-Sample Heterogeneity) package in R [36]. The cis-meQTL test for association of nearby SNPs with DNA methylation measurements was carried out using the MatrixEQTL R package (v2.3) [52], with covariate adjustment for sex, and the five principal components of methylation array control probes and genotyping array ancestry estimates.

Data management and deposition

Data management for this project utilized a centralized cloud computing-based management approach as previously described [53, 54]. Using quality control (QC) procedures for clinical, immunologic and epigenetic data, we implemented rigorous checks to ensure the reliability and accuracy of the datasets. Quality assurance (QA) involved systematic processes to validate the integrity and consistency of the generated data. This included verifying data completeness across datasets, conducting checks for accuracy and ensuring adherence to predefined standards. We also addressed potential issues, such as missing values, outliers and discrepancies.

Supplementary Information

The online version contains supplementary material available at https://doi.org/10.1186/s13148-024-01703-0.

Additional file 1. Supplementary Figures S1 and S2.

Additional file 2. Full list of IDEAL consortium authors.

Additional file 3. Table S2 - Table of statistics for genome-wide significant IAP-associated differentially methylated regions.

Additional file 4.Table S3 - Table of statistics for genome-wide significant MPL-associated differentially methylated regions.

Acknowledgements

We wish to acknowledge the Australian Genome Research Facility Genotyping service team for their service. OL, SvH and JDA acknowledge Drs. Gary Fleisher, Wendy Chung, Nancy Andrews and Kevin Churchwell of Boston Children's Hospital for their support of the *Precision Vaccines Program*.

Author contributions

OL, MP, DM, JS, SvH helped in conception/design of the work; SVH, RK, NK, MP collected the data; JDA and AH contributed to data management and quality assurance; DM, NS analyzed the data; all authors helped in critical revisions; OL, MP were involved in final approvals.

Funding

This study was funded in part via NIH NIAID Immune Development in Early Life (IDEAL) U19AI168643. OL's laboratory is also supported by Adjuvant Discovery Program and Adjuvant Development Program contracts 75N93019C00044 and HHSN272201800047C, respectively. JL-S is further supported by R01HL123915 and R01HL155742.

Availability of data and materials

Following the de-identification and QC/QA processes, the data were securely deposited into ImmPort under accession number SDY2506. All analysis codes have been deposited at Bitbucket https://bitbucket.org/pvp-dmac/ideal_

pilot/src/main/ and are publicly available as of the date of publication. Any additional information required to reanalyze the data reported in this paper is available from the lead contact upon request.

Declarations

Ethics approval and consent to participate

The study ethics and protocol were approved by The Rochester Regional Health Human Subjects Review Board under the approval number CIC 1141-B-09-1.

Consent for publication

All authors have agreed to publish this manuscript on Clinical Epigenetics.

Competing interests

JL-S is a scientific advisor to Precion Inc. and TruDiagnostic Inc. OL and SvH are named inventors on patents related to vaccine adjuvants and human in vitro systems that model immune responses. Their laboratories have received a sponsored research agreement from GlaxoSmithKline (GSK). OL is a co-founder of *Ovax* LLC.

Received: 25 March 2024 Accepted: 30 June 2024
Published online: 03 July 2024

References

1. WHO. Neonatal Mortality Rate (SDG 3.2.2). In: The Global Strategy for Women's, Children's and Adolescents' Health (2016-2030). 2015.
2. Pichichero ME, Casey JR, Almudevar A, Basha S, Surendran N, Kaur R, et al. Functional immune cell differences associated with low vaccine responses in infants. J Infect Dis. 2016;213(12):2014–9.
3. Morris MC, Almudevar AL, Casey JR, Pichichero ME. Familial and microbiological contribution to the otitis-prone condition. Int J Pediatr Otorhinolaryngol. 2015;79(12):2174–7.
4. Pichichero ME, Casey JR, Almudevar A. Nonprotective responses to pediatric vaccines occur in children who are otitis prone. Pediatr Infect Dis J. 2013;32(11):1163–8.
5. Chapman TJ, Morris MC, Xu L, Pichichero ME. Nasopharyngeal colonization with pathobionts is associated with susceptibility to respiratory illnesses in young children. PLoS ONE. 2020;15(12): e0243942.
6. Pichichero ME, Chapman TJ, Bajorski P. Pneumonia, sinusitis, influenza and other respiratory illnesses in acute otitis media-prone children. Pediatr Infect Dis J. 2021;40(11):975–80.
7. Pichichero ME. Immunologic dysfunction contributes to the otitis prone condition. J Infect. 2020;80(6):614–22.
8. Basha S, Kaur R, Mosmann TR, Pichichero ME. Reduced T-Helper 17 Responses to Streptococcus pneumoniae in Infection-Prone Children Can Be Rescued by Addition of Innate Cytokines. J Infect Dis. 2017;215(8):1321–30.
9. Mersha TB, Afanador Y, Johansson E, Proper SP, Bernstein JA, Rothenberg ME, et al. Resolving clinical phenotypes into endotypes in allergy: molecular and omics approaches. Clin Rev Allergy Immunol. 2021;60(2):200–19.
10. Perrem L, Subbarao P. Moving the dial on identifying endotypes of asthma from early life. Eur Respir J. 2022;60(3).
11. Martino DJ, Tulic MK, Gordon L, Hodder M, Richman TR, Metcalfe J, et al. Evidence for age-related and individual-specific changes in DNA methylation profile of mononuclear cells during early immune development in humans. Epigenetics. 2011;6(9):1085–94.
12. Martino DJ, Saffery R, Allen KJ, Prescott SL. Epigenetic modifications: mechanisms of disease and biomarkers of food allergy. Curr Opin Immunol. 2016;42:9–15.
13. Pech M, Weckmann M, König IR, Franke A, Heinsen FA, Oliver B, et al. Rhinovirus infections change DNA methylation and mRNA expression in children with asthma. PLoS ONE. 2018;13(11): e0205275.
14. Elgizouli M, Logan C, Grychtol R, Rothenbacher D, Nieters A, Heinzmann A. Reduced PRF1 enhancer methylation in children with a history of severe RSV bronchiolitis in infancy: an association study. BMC Pediatr. 2017;17(1):65.
15. DiNardo AR, Netea MG, Musher DM. Postinfectious epigenetic immune modifications: a double-edged sword. N Engl J Med. 2021;384(3):261–70.
16. Novakovic B, Habibi E, Wang SY, Arts RJW, Davar R, Megchelenbrink W, et al. beta-glucan reverses the epigenetic state of LPS-induced immunological tolerance. Cell. 2016;167(5):1354–68.
17. Lee A, Wimmers F, Pulendran B. Epigenetic adjuvants: durable reprogramming of the innate immune system with adjuvants. Curr Opin Immunol. 2022;77: 102189.
18. Cotugno N, Ruggiero A, Santilli V, Manno EC, Rocca S, Zicari S, et al. OMIC technologies and vaccine development: from the identification of vulnerable individuals to the formulation of invulnerable vaccines. J Immunol Res. 2019;2019:8732191.
19. Pichichero ME, Xu L, Gonzalez E, Pham M, Kaur R. Variability of vaccine responsiveness in young children. J Infect Dis. 2023.
20. Tian E, Syed ZA, Edin ML, Zeldin DC, Ten Hagen KG. Dynamic expression of mucins and the genes controlling mucin-type O-glycosylation within the mouse respiratory system. Glycobiology. 2023;33(6):476–89.
21. Bonser LR, Erle DJ. Airway Mucus and Asthma: The Role of MUC5AC and MUC5B. J Clin Med. 2017;6(12).
22. Suzuki S, Morishima S, Murata M, Tanaka M, Shigenari A, Ito S, et al. Sequence variations within HLA-G and HLA-F genomic segments at the human leukocyte antigen telomeric end associated with acute graft-versus-host disease in unrelated bone marrow transplantation. Front Immunol. 2022;13: 938206.
23. Shi K, Ge MN, Chen XQ. Coordinated DNA methylation and gene expression data for identification of the critical genes associated with childhood atopic asthma. J Comput Biol. 2020;27(1):109–20.
24. Jiang H, Li Y, Shen M, Liang Y, Qian Y, Dai H, et al. Interferon-α promotes MHC I antigen presentation of islet β cells through STAT1-IRF7 pathway in type 1 diabetes. Immunology. 2022;166(2):210–21.
25. Zhao X, Zhang X, Wu Z, Mei J, Li L, Wang Y. Up-regulation of microRNA-135 or silencing of PCSK6 attenuates inflammatory response in preeclampsia by restricting NLRP3 inflammasome. Mol Med. 2021;27(1):82.
26. Shi W, Jin M, Chen H, Wu Z, Yuan L, Liang S, et al. Inflammasome activation by viral infection: mechanisms of activation and regulation. Front Microbiol. 2023;14:1247377.
27. Wei H, Wang D, Qian Y, Liu X, Fan S, Yin HS, et al. Structural basis for the specific recognition of IL-18 by its alpha receptor. FEBS Lett. 2014;588(21):3838–43.
28. Ma L, Li W, Zhang Y, Qi L, Zhao Q, Li N, et al. FLT4/VEGFR3 activates AMPK to coordinate glycometabolic reprogramming with autophagy and inflammasome activation for bacterial elimination. Autophagy. 2022;18(6):1385–400.
29. Lin J, Harding A, Giurisato E, Shaw AS. KSR1 modulates the sensitivity of mitogen-activated protein kinase pathway activation in T cells without altering fundamental system outputs. Mol Cell Biol. 2009;29(8):2082–91.
30. Higashi H, Maejima T, Lee LH, Yamazaki Y, Hottiger MO, Singh SA, et al. A study into the ADP-ribosylome of IFN-γ-stimulated THP-1 human macrophage-like cells identifies ARTD8/PARP14 and ARTD9/PARP9 ADP-ribosylation. J Proteome Res. 2019;18(4):1607–22.
31. Kurebayashi Y, Nagai S, Ikejiri A, Ohtani M, Ichiyama K, Baba Y, et al. PI3K-Akt-mTORC1-S6K1/2 axis controls Th17 differentiation by regulating Gfi1 expression and nuclear translocation of RORγ. Cell Rep. 2012;1(4):360–73.
32. Lannoy V, Côté-Biron A, Asselin C, Rivard N. TIRAP, TRAM, and toll-like receptors: the untold story. Mediators Inflamm. 2023;2023:2899271.
33. Lu SC. Glutathione synthesis. Biochim Biophys Acta. 2013;1830(5):3143–53.
34. Smith RL, Soeters MR, Wüst RCI, Houtkooper RH. Metabolic flexibility as an adaptation to energy resources and requirements in health and disease. Endocr Rev. 2018;39(4):489–517.
35. Zhang H, Liu J, Yang Z, Zeng L, Wei K, Zhu L, et al. TCR activation directly stimulates PYGB-dependent glycogenolysis to fuel the early recall response in CD8(+) memory T cells. Mol Cell. 2022;82(16):3077-88.e6.
36. Zheng SC, Breeze CE, Beck S, Teschendorff AE. Identification of differentially methylated cell types in epigenome-wide association studies. Nat Methods. 2018;15(12):1059–66.
37. Pichichero ME. Ten-year study of acute otitis media in rochester. NY Pediatr Infect Dis J. 2016;35(9):1027–32.

38. Welsh KG, Rousseau K, Fisher G, Bonser LR, Bradding P, Brightling CE, et al. MUC5AC and a glycosylated variant of MUC5B alter mucin composition in children with acute asthma. Chest. 2017;152(4):771–9.
39. Pichichero ME, Almudevar A. Inflammation-associated cytokine analysis identifies presence of respiratory bacterial pathogens in the nasopharynx. Pathog Dis. 2016;74(6).
40. Ren D, Xu Q, Almudevar AL, Pichichero ME. Impaired proinflammatory response in stringently defined otitis-prone children during viral upper respiratory infections. Clin Infect Dis. 2019;68(9):1566–74.
41. Surendran N, Nicolosi T, Pichichero M. Infants with low vaccine antibody responses have altered innate cytokine response. Vaccine. 2016;34(47):5700–3.
42. Verhoeven D, Nesselbush M, Pichichero ME. Lower nasopharyngeal epithelial cell repair and diminished innate inflammation responses contribute to the onset of acute otitis media in otitis-prone children. Med Microbiol Immunol. 2013;202(4):295–302.
43. Verhoeven D, Pichichero ME. Divergent mucosal and systemic responses in children in response to acute otitis media. Clin Exp Immunol. 2014;178(1):94–101.
44. Kaur R, Casey J, Pichichero M. Differences in innate immune response gene regulation in the middle ear of children who are otitis prone and in those not otitis prone. Am J Rhinol Allergy. 2016;30(6):218–23.
45. Hannon E, Gorrie-Stone TJ, Smart MC, Burrage J, Hughes A, Bao Y, et al. Leveraging DNA-methylation quantitative-trait loci to characterize the relationship between methylomic variation, gene expression, and complex traits. Am J Hum Genet. 2018;103(5):654–65.
46. Aryee MJ, Jaffe AE, Corrada-Bravo H, Ladd-Acosta C, Feinberg AP, Hansen KD, et al. Minfi: a flexible and comprehensive Bioconductor package for the analysis of Infinium DNA methylation microarrays. Bioinformatics. 2014;30(10):1363–9.
47. McCartney DL, Walker RM, Morris SW, McIntosh AM, Porteous DJ, Evans KL. Identification of polymorphic and off-target probe binding sites on the Illumina Infinium MethylationEPIC BeadChip. Genom Data. 2016;9:22–4.
48. Chang CC, Chow CC, Tellier LC, Vattikuti S, Purcell SM, Lee JJ. Second-generation PLINK: rising to the challenge of larger and richer datasets. Gigascience. 2015;4:7.
49. Ritchie ME, Phipson B, Wu D, Hu Y, Law CW, Shi W, et al. limma powers differential expression analyses for RNA-sequencing and microarray studies. Nucleic Acids Res. 2015;43(7):e47-e.
50. Peters TJ, Buckley MJ, Statham AL, Pidsley R, Samaras K, Lord R, et al. De novo identification of differentially methylated regions in the human genome. Epigenet Chromatin. 2015;8(1):6.
51. Phipson B, Maksimovic J, Oshlack A. missMethyl: an R package for analyzing data from Illumina's HumanMethylation450 platform. Bioinformatics. 2016;32(2):286–8.
52. Shabalin AA. Matrix eQTL: ultra fast eQTL analysis via large matrix operations. Bioinformatics. 2012;28(10):1353–8.
53. Vignolo SM, Diray-Arce J, McEnaney K, Rao S, Shannon CP, Idoko OT, et al. A cloud-based bioinformatic analytic infrastructure and Data Management Core for the Expanded Program on Immunization Consortium. J Clin Transl Sci. 2020;5(1): e52.
54. IMPACC. Immunophenotyping assessment in a COVID-19 cohort (IMPACC): A prospective longitudinal study. Sci Immunol. 2021;6(62).

Publisher's Note